Journal of Solid State Chemistry **154,** 444–450 (2000)
doi:10.1006/jssc.2000.8863, available online at http://www.idealibrary.com on IDEAL®

# Sintering of Additive Free Hydrothermally Derived Indium Tin Oxide Powders in Air

C. P. Udawatte and K. Yanagisawa[1]

*Research Laboratory of Hydrothermal Chemistry, Faculty of Science, Kochi University, Akebono-cho 2-5-1, Kochi-shi 780-8520, Japan*

and

S. Nasu

*Division of Materials Physics, Department of Physical Science, School of Engineering Science, Osaka University, Toyonaka, Osaka 560–8531, Japan*

Received March 14, 2000; in revised form June 26, 2000; accepted July 13, 2000; published online September 30, 2000

**High-density and chemically homogeneous Sn-doped (0–10 mole%) indium oxide (ITO) ceramics have been successfully prepared using a highly sinterable hydrothermally derived In–Sn oxyhydroxide fine powder as the starting material. Low-temperature calcination at 500°C of the hydrothermally prepared phase led to formation of a substitutional vacancy type solid solution of $In_2Sn_{1-x}O_{5-y}$. The sintering behavior of the calcined powder compacts was studied at temperatures from 1200 to 1500°C for 3 h in air. C-type rare-earth oxide structured ITO ceramics were obtained with fine microstructures and fewer pores. Neither the $O_2$ sintering atmosphere nor sintering aids were used to promote the densification of ITO ceramics. It was found that the addition of Sn to $In_2O_3$ propelled the densification.** 

*Key Words:* **calcination; density; hydrothermal; ITO; Mössbauer; SEM; sintering.**

## INTRODUCTION

Sn-doped indium oxide, commonly called ITO, is technologically important and is widely used as a transparent conducting oxide in electronic and opto-electronic devices due to its excellent properties of high conductivity ($10^4\ \Omega^{-1}\ cm^{-1}$) and high transparency (85–90%) to visible light (1–3). The ITO thin films are commonly deposited by the magnetron sputtering method using either In–Sn alloy or $In_2O_3$–$SnO_2$ oxide as the sputtering target. However, it was reported (4) that an oxide target is easier to use than a metallic one due to its lower sensitivity to minor changes in sputtering parameters. The sputtering efficiency and properties of the sputtered films strongly depend on the characteristics of the sputtering targets (4, 5). Dense targets increase the deposition rates and exhibit a more stable resistivity of the deposited films (6).

At normal pressure, $In_2O_3$ has a C-type rare-earth oxide (cubic) structure with the space group of $T_h^7$ la3 (7). The lattice parameter is 10.117(1) Å, which gives a theoretical density (TD) of 7.120 g $cm^{-3}$ (7). The coordination is sixfold for In atoms and fourfold for O atoms (7). The sixfold In atoms fall into two different crystallographically nonequivalent coordinated sites. One-fourth of the cations are in trigonally compressed octahedra, and the remaining three-fourths are in highly distorted octahedra (7). A small amounts of Sn atoms can enter substitutionally in the cation sublattice to be described as $In_{2-y}Sn_yO_3$ or $In_{2-y}Sn_yO_{3-2x}$ (3).

Densification of $In_2O_3$ is very difficult due to sublimation of In at high temperatures (8). This sublimation problem, together with many undesirable features such as nonstoichiometry and wide fluctuations in composition due to loss of Sn and In at high temperatures, might result in poor densification of ITO. Bates *et al.* (9) reported that the relative density of sintered ITO ceramics is in the range of 62–65% after sintering under normal atmospheric conditions, but sintering in an oxidizing atmosphere gave fully densified bodies (4). However, sintering in an oxidizing atmosphere is dangerous and requires an expensive and complex furnace. It is also reported that a few percent of additives such as $SiO_2$, $TiO_2$, and $Bi_2O_3$ increase the densification (4–6, 10). Nevertheless, if the additives remain in the sintered ITO ceramics, it could have a negative impact on the properties of the sputtered films.

[1]To whom correspondence should be addressed. Tel.: +81 88 844 8350. Fax: +81 88 844 8362. E-mail: yanagi@cc.kochi.-u.ac.jp.



0022-4596/00 $35.00

Our studies were focussed on fabricating additive-free dense ITO targets in air as the sintering atmosphere. In this process, well-crystallized Sn-doped InOOH fine powders were prepared by hydrothermally treating a coprecipitated In–Sn amorphous gel, and then the derived phase was calcined at 500°C in air to form $In_2Sn_{1-x}O_{5-y}$. Using the calcined powder, a dense ITO target (~93% TD) with a mole ratio of In:Sn 95:5 was fabricated (11). The paramount goal of the present investigation is to determine the sintering behavior of the hydrothermally prepared ITO powders with a wide range of Sn contents at relatively low temperatures in air.

## EXPERIMENTAL

The experimental procedure described in our previous report (12) was employed to prepare the Sn-doped InOOH powders. The coprecipitated gels with a mole ratio of Sn/(In + Sn) from 0 to 0.1 were hydrothermally treated in an ammonia solution (pH 9) at 300°C for 24 h to obtain the above-mentioned phase.

The powders thus formed were used as starting materials to fabricate the ITO targets. First, the dried powders were calcined at 500°C for 1 h in air and ground well using an agate mortar. About 0.5 g of the ground powders was mixed with a binder (1 wt% stearic acid) in order to improve the compacting behavior. The powders were then uniaxially pressed in a hardened steel die into pellets (10 mm in diameter; ~1.5 mm in thickness) at 150 MPa. All the compacts had bulk green densities ranging from 45% to 50% of TD. The compacted pellets were then sintered in air at 1200 to 1500°C for 3 h on a zirconia plate at a heating rate of 4°C/min. After the sintering the samples were allowed to cool as the furnace cooled. The bulk density of the sintered pellet was determined by geometrical estimation, while the apparent density was evaluated by Archimedes' method in water.

Compositional analyses were performed at each step in the process (coprecipitation, hydrothermal treatment, calcination, and sintering) for every sample by using an inductively coupled plasma electron spectrometer (ICPS-SPS 7000A-SII Seiko Instruments Inc., Tokyo, Japan) after the samples were dissolved in a concentrated HCl solution. In order to study the environment of tin in the process, the samples were subjected to a $^{119}$Sn Mössbauer spectroscopic investigation at room temperature. The Mössbauer spectrometer used is a commercial set up supplied by Wissel-GmbH (Hamburg, Germany) and operated in a constant acceleration mode. The details of the Mössbauer measurement have been described elsewhere (12). The obtained crystalline phases of the samples were identified by X-ray diffraction (XRD) measurements (Rigaku-Rotaflex, Tokyo, Japan) made on an instrument equipped with a graphite monochlometer using Cu$K\alpha$ radiation. For the unit cell parameter measurements, XRD data of seven reflections (222, 400, 411, 332, 510, 431, and 440) of ITO ceramics were collected with a Si internal standard using a slow scan speed (0.001° ($2\theta$)/s). Lattice parameters were determined by a least-squares method. The standard deviation of each sample was approximately $10^{-3}$ Å. Microstructure observations of the fractured surfaces of the ITO ceramics sintered at different temperatures were performed using scanning electron microscopy (SEM, Hitachi-H-530, Tokyo, Japan).

## RESULTS AND DISCUSSION

Broad XRD peaks with low intensity were observed in all In–Sn coprecipitated gels, and were similar to the pattern of pure $In(OH)_3$ gel. The absences of well-defined rings in the diffraction patterns by TEM analysis confirmed that the gels are substantially amorphous. Hydrothermal treatment of the coprecipitated gel without Sn at 300°C for 24 h resulted in formation of InOOH with a trace of $In(OH)_3$, but the Sn-doped gels led to the formation of a single phase of Sn-doped InOOH (Fig. 1A). The crystallinity of the hydrothermally derived Sn-doped InOOH phases decreased with increasing Sn content. A shift of the peak position toward the higher angle side in the XRD patterns was observed upon the addition of a small amount of Sn (3%), but the peak shifted again toward the lower angle side with further increases of the Sn content.

The calcination of the pure InOOH phase at 500°C gave a $In_2O_3$ phase with C-type rare-earth oxide structure (Fig. 1B-a), but calcination of the Sn-doped InOOH phase gave a substitutional vacancy type interstitial solid solution of $In_2Sn_{1-x}O_{5-y}$ (Figs. 1B-b–B-e). The crystallinity of the calcined products typically declined with the Sn content.

Further heating of these $In_2Sn_{1-x}O_{5-y}$ phases above 1000°C resulted in formation of a Sn-doped $In_2O_3$ phase, which had the same structure as that with pure $In_2O_3$ (13). The XRD patterns (Fig. 1C) of the ITO specimens sintered at 1450°C for 3 h showed the formation of a single phase of cubic Sn-doped $In_2O_3$. A shift of the peak positions toward the lower angle side was observed in the sample with low Sn content (Figs. 1C-b and 1C-c), compared with the peak for the pure $In_2O_3$ phase (Fig. 1C-a), due to the lattice parameter increase caused by Sn substitution. However, further increasing the Sn content caused a shift in the peaks toward the higher angle side.

The observed lattice parameters for the sintered ITO (1450°C for 3 h) versus the tin content determined by the chemical analyses are shown in Fig. 2. The lattice parameter of pure $In_2O_3$ ceramics sintered at 1450°C was determined to be $a_0 = 10.1169(1)$ Å, which agreed with the reported value of 10.1170(1) Å (7). An abrupt increment of the lattice parameter was observed even with just a few percent of tin doping. These results are very similar to the reported data

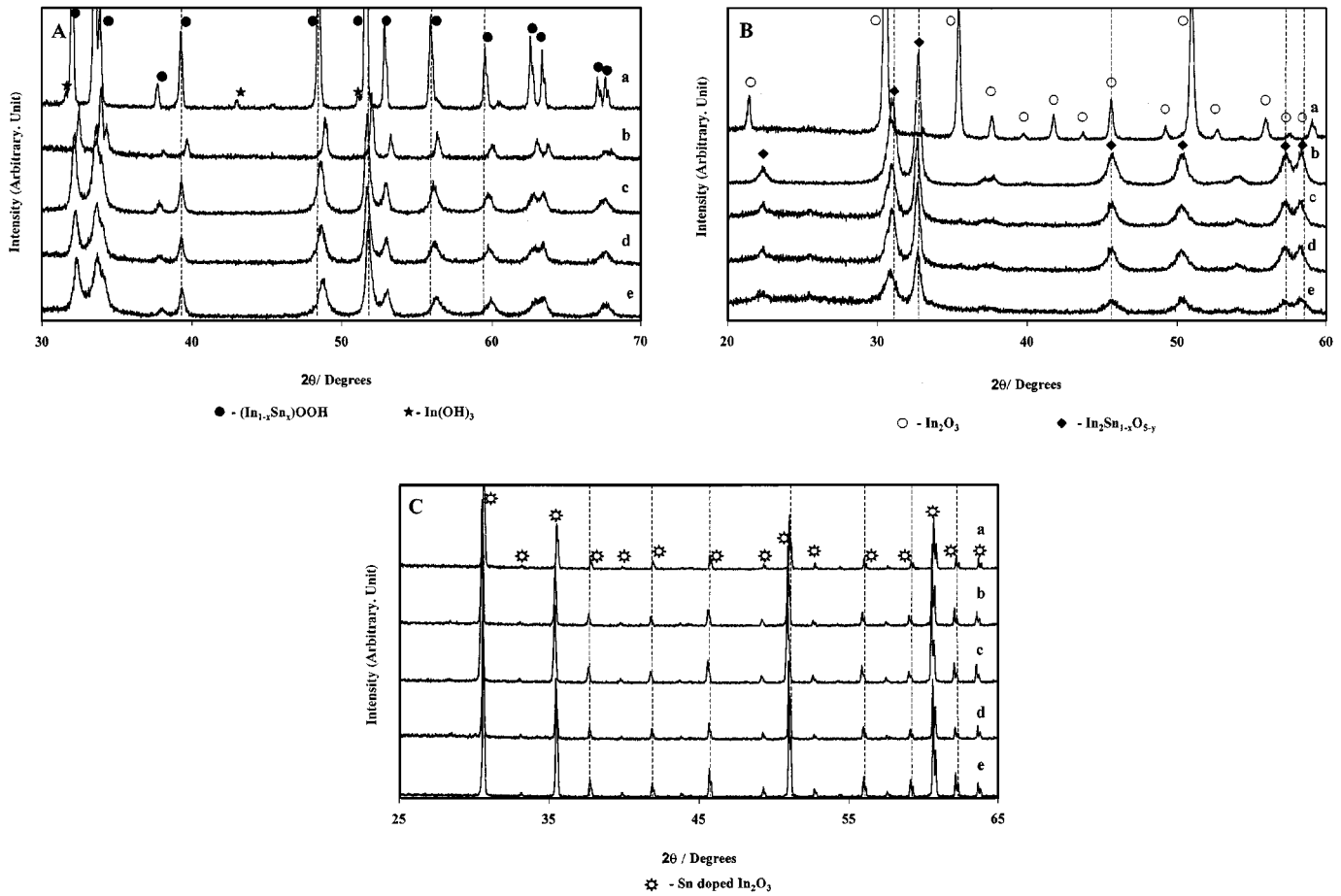


**FIG. 1.** XRD patterns of ITO powders: (A) after hydrothermal treatment at 300°C for 24 h; (B) after calcination at 500°C for 1 h; and (C) after sintering at 1450°C for 3 h. For all a, 0 mole% Sn; b, 3 mole% Sn; c, 5 mole% Sn; d, 7 mole% Sn; and e, 10 mole% Sn.

(14), but both present and reported results disagree with the generally accepted concept of a linear decrease in the lattice parameter (unless there is a disorder site in the lattice) as the tin content increases, because the $Sn^{4+}$ ionic radius (0.71 Å) is smaller than that of $In^{3+}$ (0.81 Å). This observed effect could be due to the opening of more oxygen vacancies with increasing tin content. However, the lattice parameter reached the maximum limit at a tin content of 5 mole%, which is slightly lower than the solubility limit (7%) reported by Nadaud *et al.* (14). Further increases in the sintering temperature (> 1450°C) resulted in a slight decrease of the cell parameter, presumably because of the loss of Sn.

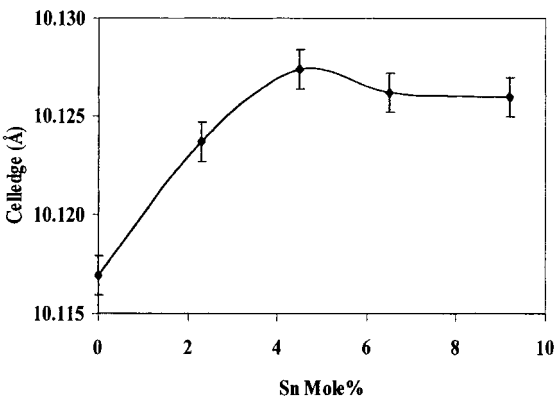


**FIG. 2.** Lattice parameter of ITO ceramics sintered at 1450°C for 3 h as a function of Sn content.

A color change was also observed during the process. The yellow-colored In–Sn hydrated gel changed to white after the hydrothermal treatments, and then turned to yellow again with the calcination. Finally, it turned to dark green or black after the sintering.

The relative bulk densities and the weight losses of the sintered bodies as a function of sintering temperature are shown in Figs. 3A and 3B, respectively. For the pure $In_2O_3$ (Fig. 3A-a), its highest bulk density, 84% of TD, was obtained after sintering at 1500°C. For Sn-doped $In_2O_3$, the bulk density increased as the temperature increased from

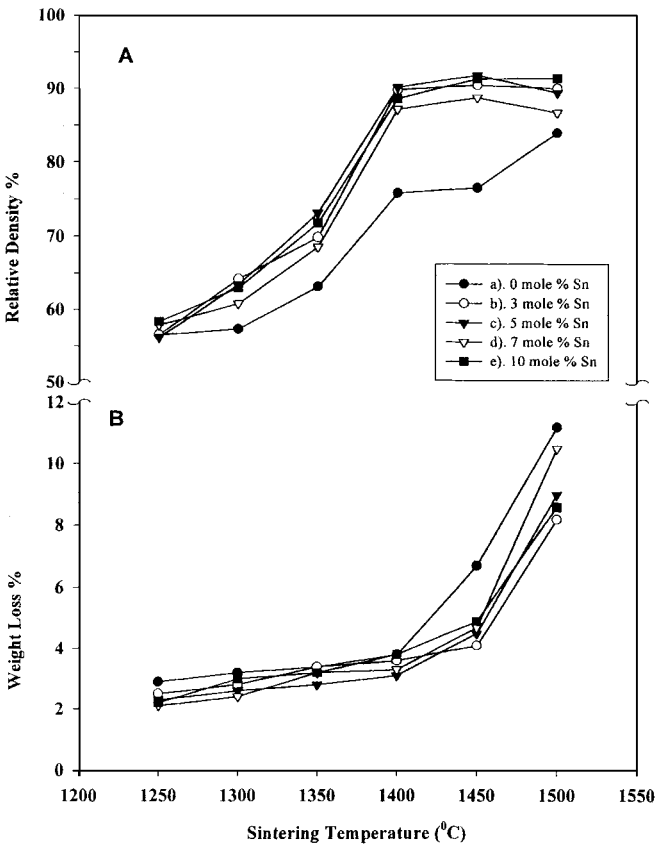


**FIG. 3.** Densification of $In_2O_3$ composites with and without Sn, sintered in air at selected temperatures for 3 h: (A) relative density and (B) weight loss.

1250 to 1450°C, where it maximized. The sintering temperature of 1450°C, which gave a maximum sintered density (~92% of TD), is lower than that usually used for either sintering in an oxidized atmosphere or with additives. However, the amount of tin content does not lead to a significant difference in the relative densities obtained at 1450°C, which fall in the range of 88–92%. The apparent densities of the ITO ceramics sintered at 1400°C and 1450°C were determined in the range of 97–98% of TD, which indicated the presence of dominant open pores. The degree of increase of the sintered density at temperatures below 1400°C is larger than that at higher temperatures in all Sn-doped samples, showing that the sintering occurs mainly between 1300–1400°C.

The weight losses observed after sintering of each ITO ceramic are shown in Fig. 3B. They included 1% organic binder decomposition. Generally, materials with higher densities have smaller weight losses. However, the results in Figs. 3A and 3B show a slight decrease in bulk densities of all ITO ceramics at 1500°C with weight losses in the range of 8–10%. The weight loss during the sintering at 1450°C is ~4.5% in all cases (Fig. 3B).

According to the chemical analyses, the mole ratio of In:Sn in the prepared gels and their hydrothermally treated and calcined powders remained same as their starting values, showing no loss of In or Sn during the process. However, a slight loss of Sn (2–3 wt% from total Sn) was observed in the ITO ceramics after the sintering process at high temperatures over 1450°C.

The preliminary densification of ITO occurred at 1000–1200°C due to the phase change from $In_2Sn_{1-x}O_5$ to cubic $In_{2-y}Sn_yO_3$ (11) and resulted in necking of the particles. The fracture surfaces of the selected ITO materials (5 mole% Sn) sintered in air at various temperatures are shown in Fig. 4. As the sintering temperature increased, the grain sizes increased and a remarkable grain growth occurred at 1250°C. A reasonably high degree of densification with fairly uniform grain sizes in the range of 2–3 μm was observed for the material synthesized at 1300°C. At 1350°C the particles took a well-faceted morphology. The ceramics sintered at 1400°C showed a dense fracture surface with enhanced grain size of 4–5 μm together with a few small pores. The highest densification was observed at 1450°C (Fig. 4e) with grain size up to ~7 μm having fewer pores, which were mainly located at the triple grain junction and were rarely found within the grain. The material sintered at 1500°C showed (Fig. 4f) an abnormal grain growth, having a wide range in sizes (4–10 μm). The microstructures of the other ITO ceramics with different Sn contents also showed behavior similar to that in the presented micrographs (5 mole% Sn), but pure $In_2O_3$, which was sintered under the same conditions at 1450°C, showed small grain sizes (3–4 μm) with a significant amount of open pores (Fig. 5a). The pure $In_2O_3$ sintered at 1500°C for 3 h, where it reached the maximum density, showed (Fig. 5b) grain growth similar to those observed for the ITO ceramics. Thus, the presence of even a small amount of Sn abruptly increased the densification of $In_2O_3$.

The Mössbauer spectrum of the coprecipitated In–Sn gel (Fig. 6a) showed a singlet (with isomer shift, IS, $\delta = -0.04$ mm/sec) and a weak doublet (marked with "↓") having $\delta = 2.86$ and quadrupole shift (QS) $\Delta = 1.5$ mm/sec, which correspond to 96% $Sn^{4+}$ and 4%$Sn^{2+}$. During the hydrothermal process, the remaining $Sn^{2+}$ oxidized to $Sn^{4+}$ and occupies the perfect In site in the InOOH lattice, as evidenced by a single peak in the respective Mössbauer spectrum (Fig. 6b) with a value of $\delta = 0$ mm/sec. The Mössbauer analysis (Fig. 6c) of the calcined powder (at 500°C for 3 h) again confirmed that the oxidation state of Sn is $4^+$ in a perfect octahedral site with $\delta = 0$ mm/sec. The observed spectrum is very similar to that reported for $In_2SnO_5$ with $\delta = 0$ mm/sec (15). Quadrupole splitting arose in the spectrum of the sintered ITO ceramic (5 mole% Sn; Fig. 6d), since the Mössbauer-active Sn was surrounded by noncubic extranuclear fields. Therefore, the spectrum was fitted into two doublets having isomer shifts of 0.14 and 0.15 mm/sec

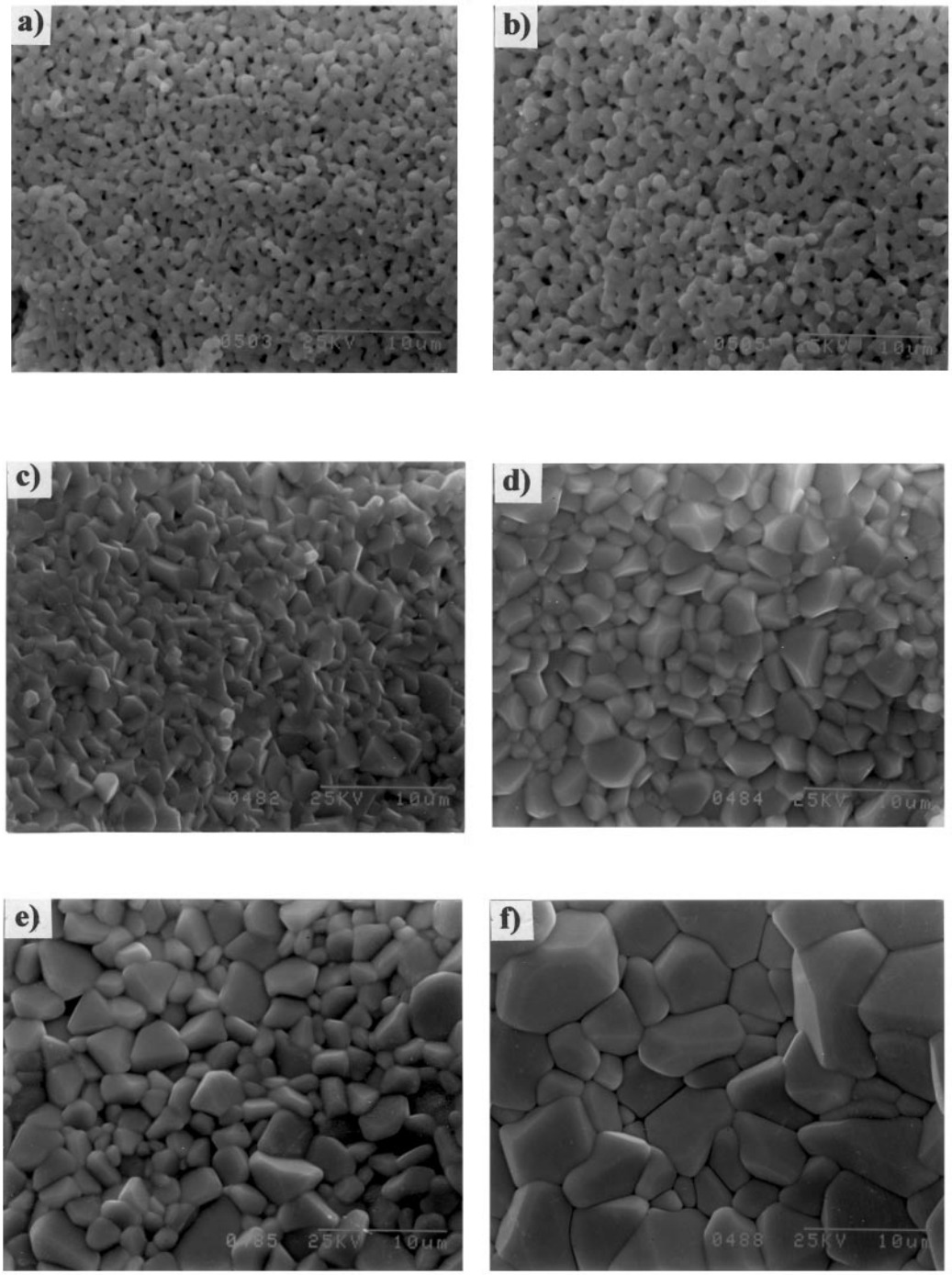


**FIG. 4.** SEM micrographs of the fractured surface of the ITO ceramics sintered in air at (a) 1250°C, (b) 1300°C, (c) 1350°C, (d) 1400°C, (e) 1450°C, and (f) 1500°C for 3 h.

and quadrupole splittings of 1.18 and 0.52 mm/sec, respectively. These observed Mössbauer parameters for tetravalent Sn are very similar to the data reported by Nadaud *et al*. (14). The doped Sn atoms may occupy both ordered and disordered $In^{3+}$ sites in the $In_2O_3$ lattice with almost equal probability. The presence of Sn in the $In_2O_3$ lattice caused more distortion of the lattice, which could be one reason for the increase in the cell parameter with Sn doping. The measured Mössbauer spectra of other ITO-sintered bodies (3, 7, and 10 mole% Sn) are also similar to the reported spectrum but the QS increases with increasing tin content.

## CONCLUSIONS

The Sn-doped indium oxide fine powders prepared by hydrothermal and post annealing methods are highly sinterable. Well-densified ITO ceramics (3–10 mole% Sn) were fabricated in air using densely packed green compacts. The sintering mainly occurred between 1300–1400°C. The maximum densification was observed after sintering at 1450°C for 3 h. The bulk density of such ITO ceramics was in the range of 90–92% of the theoretical density. The ceramics had uniform and fine-grained microstructures. The doping element Sn promoted the densification of $In_2O_3$. The substituted Sn atoms occupied both ordered and disordered $In^{3+}$ sites in the C-type rare-earth oxide structured $In_2O_3$ lattice.

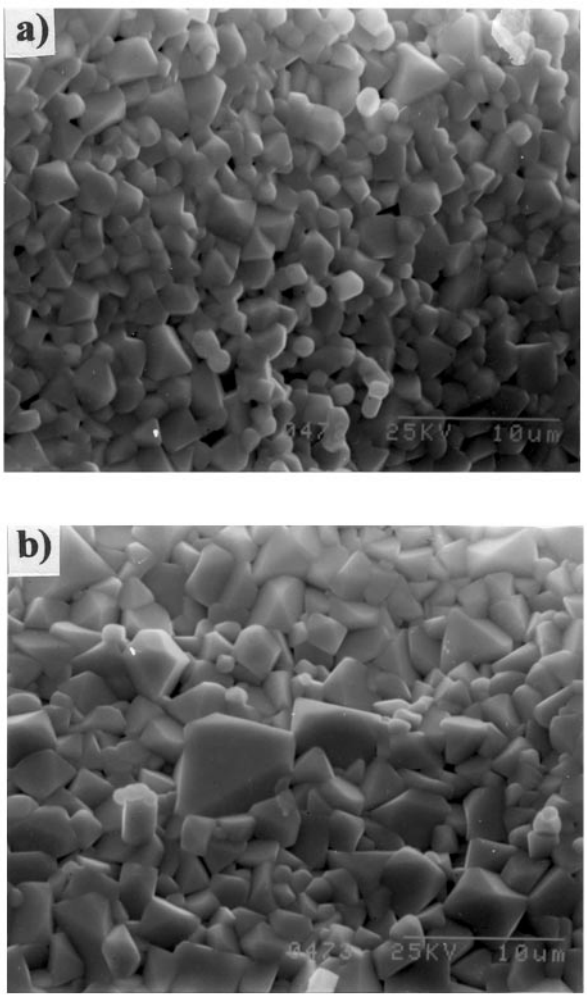


**FIG. 5.** SEM micrographs of the fractured surface of the pure $In_2O_3$ ceramics sintered in air at (a) 1450°C and (b) 1500°C for 3 h.

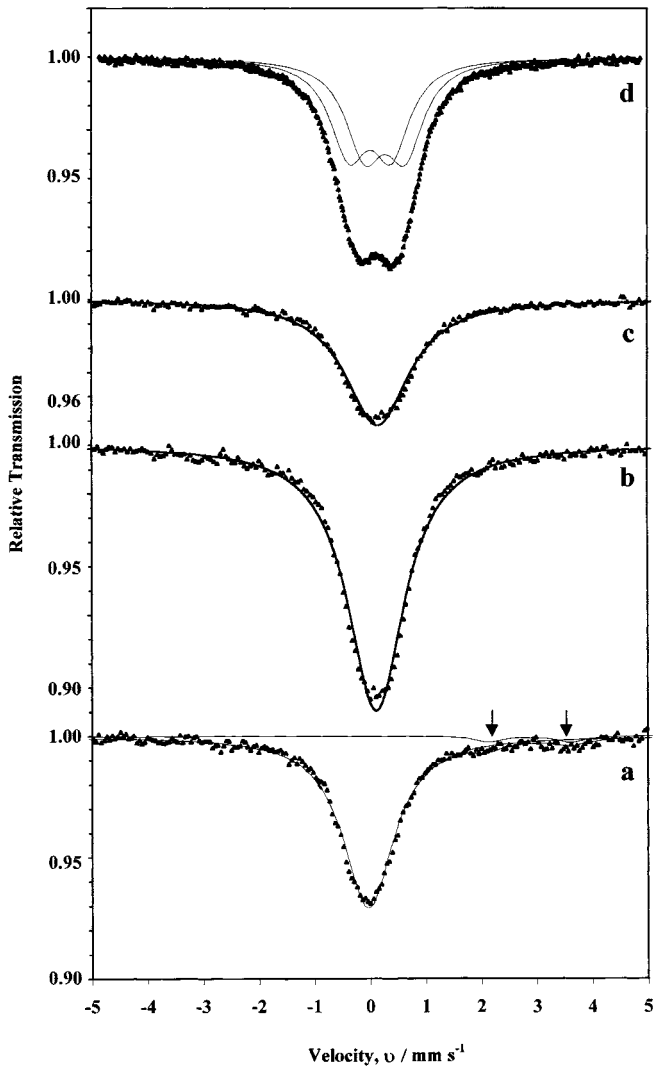


**FIG. 6.** Room temperature Mössbauer spectra of ITO powders: (a) In–Sn coprecipitated gel; (b) after hydrothermal treatment at 300°C for 24 h; (c) after calcination at 500°C for 1 h; and (d) after sintering at 1450°C for 3 h.

## ACKNOWLEDGMENTS

C.P.U. thanks MONBUSHO-Japan for awarding a Post Doctoral Research Position to work in Japan.

## REFERENCES

1. J. J. Vossen, *Phys. Thin Films* **9,** 1 (1977).
2. N. Balasubramanian and A. Subrahamanyam, *J. Electrochem. Soc.* **138,** 322 (1991).
3. I. Hamberg and C. G. Graniqvist, *J. Appl. Phys.* **60,** R123 (1986).
4. N. Nadaud, M. Nanot, and P. Boch, *J. Am. Cerem. Soc.* **77,** 843 (1994).
5. B. L. Gehman, S. Jonsson, T. Rudolph, M. Scherer, M. Weight, and R. Werner, *Thin Solid Films* **220,** 333 (1992).

6. T. Vojnovich and R. J. Bartton, *Ceram. Bull.* **54,** 216 (1992).
7. M. Marezio, *Acta Crystallogr.* **20,** 723 (1966).
8. J. H. W. de Wit, *J. Solid State Chem.* **13,** 192 (1975).
9. J. L. Bates, C. W. Griffin, D. D. Marchant, and J. E. Gernier, *Am. Ceram. Soc. Bull.* **65,** 673 (1996).
10. M. Muraoka, M. Suzuki, Y. Sawada, and J. Matsushita, *J. Mater. Sci.* **33,** 5621 (1998).
11. C. P. Udawatte and K. Yanagisawa, *J. Am. Ceram. Soc.*, submitted (1999).
12. K. Yanagisawa, C. P. Udawatte, and S. Nasu, *J. Mater. Res.* **15,** 1404 (2000).
13. Joint Committee on Powder Diffraction Standards (JCPDS), Card No. 6-0416.
14. N. Naduad, N. Lequeux, M. Nanot, J. Jove, and T. Roisnel, *J. Solid State Chem.* **135,** 140 (1998).
15. M. B. Varfolomeev, A. S. Mironova, F. Kh. Chibirova, and V. E. Plyushchev, *Izv. Akad. Nauk SSSR, Neorg. Mater.* **11,** 2242 (1975).